

# Dual Recruitment of Cdc48 (p97)-Ufd1-Npl4 Ubiquitin-selective Segregase by Small Ubiquitin-like Modifier Protein (SUMO) and Ubiquitin in SUMO-targeted Ubiquitin Ligase-mediated Genome Stability Functions<sup>\*S</sup>

Received for publication, May 9, 2012, and in revised form, June 15, 2012. Published, JBC Papers in Press, June 22, 2012, DOI 10.1074/jbc.M112.379768

Minghua Nie<sup>‡</sup>, Aaron Aslanian<sup>§¶</sup>, John Prudden<sup>‡</sup>, Johanna Heideker<sup>‡</sup>, Ajay A. Vashisht<sup>||</sup>, James A. Wohlschlegel<sup>||</sup>, John R. Yates III<sup>§</sup>, and Michael N. Boddy<sup>†1</sup>

From the <sup>‡</sup>Department of Molecular Biology, The Scripps Research Institute, La Jolla, California 92037, the <sup>§</sup>Department of Chemical Physiology, The Scripps Research Institute, La Jolla, California 92037, the <sup>||</sup>Department of Biological Chemistry, David Geffen School of Medicine, UCLA, Los Angeles, California 90095, and the <sup>¶</sup>Molecular and Cell Biology Laboratory, Salk Institute for Biological Sciences, La Jolla, California 92037

**Background:** SUMO-targeted ubiquitylation controls critical cellular processes, including genome stability; but effectors and mechanisms remain undefined.

**Results:** The Cdc48-Ufd1-Npl4 segregase binds SUMO and cooperates with the SUMO-targeted ubiquitin ligase (STUbL) in DNA repair.

**Conclusion:** Cdc48-Ufd1-Npl4 acts as a STUbL effector.

**Significance:** Novel dual recognition of SUMO and ubiquitin co-modified proteins likely provides selectivity and specificity in signaling by these critical factors.

Protein modification by SUMO and ubiquitin critically impacts genome stability via effectors that “read” their signals using SUMO interaction motifs or ubiquitin binding domains, respectively. A novel mixed SUMO and ubiquitin signal is generated by the SUMO-targeted ubiquitin ligase (STUbL), which ubiquitylates SUMO conjugates. Herein, we determine that the “ubiquitin-selective” segregase Cdc48-Ufd1-Npl4 also binds SUMO via a SUMO interaction motif in Ufd1 and can thus act as a selective receptor for STUbL targets. Indeed, we define key cooperative DNA repair functions for Cdc48-Ufd1-Npl4 and STUbL, thereby revealing a new signaling mechanism involving dual recruitment by SUMO and ubiquitin for Cdc48-Ufd1-Npl4 functions in maintaining genome stability.

Posttranslational modifications regulate diverse biological processes, and cross-talk among different posttranslational modifications fine-tunes and increases the complexity of cellular regulation. For example, phosphorylation, ubiquitylation, and sumoylation all contribute extensively toward the precise orchestration of the DNA damage response, upon which both cell viability and suppression of human disease critically depend. Recent studies on the DNA damage response to DNA double strand breaks (DSBs)<sup>2</sup> link both ubiquitylation and

sumoylation to key targets at the lesion where these two modifications govern separate yet interrelated steps in DSB repair (1, 2).

A novel class of ubiquitin E3 ligases orchestrates direct cooperativity of SUMO and ubiquitin in genome maintenance. The evolutionarily conserved SUMO-targeted ubiquitin ligases (STUbLs), including human RNF4, budding yeast Slx5-Slx8, and fission yeast Rfp1/2-Slx8, catalyze the ubiquitylation of SUMO-modified proteins, which can target them for proteasome-mediated degradation (3–8). Consistent with this role, STUbL inactivation causes an accumulation of cellular SUMO-modified species, especially high molecular weight SUMO chains. Severe genomic instability and genotoxin hypersensitivity accompany the accumulation of SUMO chains, and in fission yeast, blocking SUMO chain formation mitigates these phenotypes (4, 9). The last finding suggests that either a poly-sumoylated protein(s) dominantly interferes with key cellular processes or, that the SUMO chains are themselves toxic and the critical STUbL target. Although the relevant pathways that are perturbed by STUbL inactivation remain largely undefined, STUbL maintains genome stability, at least in part, by facilitating the removal of genotoxic covalent topoisomerase I (Top1)-DNA adducts (10).

To further define the physiological impact of SUMO chains and their regulation by STUbL, we undertook a proteomics approach to identify proteins that can bind non-covalently to SUMO and/or SUMO chains in fission yeast. Intriguingly, we found the Cdc48-Ufd1-Npl4 (Cdc48-UN) protein complex was

\* This work was supported in part by National Institutes of Health Grants GM068608, GM081840 (to M.N.B.), GM093600 (to M.N.), and P41 RR011823 (to J. R. Yates III).

<sup>S</sup> This article contains supplemental Tables S1 and S2.

<sup>1</sup> Supported by a Scholar Award from the Leukemia and Lymphoma Society. To whom correspondence should be addressed: Dept. of Molecular Biology, The Scripps Research Institute, 10550 N. Torrey Pines Road, La Jolla, CA 92037. Tel.: 858-784-7042; Fax: 858-784-2265; E-mail: nboddy@scripps.edu.

<sup>2</sup> The abbreviations used are: DSB, DNA double strand break; Cdc48-UN, Cdc48-Ufd1-Npl4; SIM, SUMO interaction motif; STUbL, SUMO-targeted

ubiquitin ligase; SUMO, small ubiquitin-like modifier protein; Top1, topoisomerase I; Top1cc, Top1 cleavage complex; Tdp1, tyrosyl DNA phosphodiesterase; PCNA, proliferating cell nuclear antigen; PIP, PCNA interacting protein; DIC, differential interference contrast.

highly enriched among SUMO binding proteins. The Cdc48-UN complex is best known for its ubiquitin-mediated role in endoplasmic reticulum-associated protein degradation (11, 12). Endoplasmic reticulum-associated protein degradation substrates are extracted from the endoplasmic reticulum using the Cdc48 (human p97) AAA ATPase “motor” and directed to the proteasome for degradation. Recently, evidence for Cdc48/p97 playing key roles in the DNA damage response has emerged (11–23). Here, we define a new role for Cdc48-UN as a STUbL cofactor in protecting cells from SUMO chain-mediated toxicity, and Top1-induced genome instability. Our data suggest that Cdc48-UN can be targeted to SUMO and ubiquitin co-modified substrates such as STUbL targets via an unprecedented combination of ubiquitin and SUMO recognition motifs in Ufd1.

## EXPERIMENTAL PROCEDURES

**General Yeast Techniques**—Standard yeast methods were performed as described previously (24). Low fidelity PCR products covering the entire *ufd1* locus were used to replace the genomic locus and generate the *ufd1* temperature-sensitive (*ts*) alleles. The mutations within each mutant were identified via sequencing. Strains used in this study are listed in supplemental Table S2.

**SUMO Chain Pulldown from *Schizosaccharomyces pombe* Cell Lysate**—The *S. pombe* SUMO chains were produced in *Escherichia coli* as described (9). His<sub>6</sub>-tagged SUMO was purified from bacteria using nickel-nitrilotriacetic acid beads and eluted with 200 mM imidazole (see Fig. 1A). Purified SUMO chains were coupled to AffiGel-15 beads (Bio-Rad) in 0.1 M MOPS (pH 7.5). As a control, GST proteins were conjugated to AffiGel-10 beads in buffering containing 0.1 M HEPES, pH 6, 150 mM NaCl. Cells from the *S. pombe* SUMO deletion strain were lysed in Sp (*S. pombe*)-lysis buffer (50 mM Tris, pH 8, 150 mM NaCl, 1 mM EDTA, 10% glycerol, 0.1% Nonidet P-40, 20 mM *N*-ethylmaleimide, 2 mM PMSF, and Complete protease inhibitor EDTA-free, Roche Applied Science). Lysate containing 50 mg of proteins was pre-cleared with GST-agarose at 4 °C for 2 h to adsorb nonspecific interacting proteins and subsequently incubated with SUMO chain agarose. Both GST and SUMO beads were washed extensively with Sp-lysis buffer and eluted by competition with monomeric SUMO (see Fig. 1A).

**Fluorescence Microscopy**—To induce expression of GFP or mCherry-tagged proteins, cells were cultured in the absence of thiamine (B1) at 25 °C for 2 days. Slx8 inactivation was achieved by shifting temperature to 35 °C for 6 h. Wide-field fluorescence images of live cells were acquired using a Nikon Eclipse microscope with a 100× Plan Apochromat DIC H oil immersion objective and a Photometrics Quantix charge-coupled device camera. Images were analyzed with NIH ImageJ software.

**Chromatin Immunoprecipitation (ChIP) Assay**—Strains expressing endogenous *nmt41*:FLAG-Top1 were cultured at 25 °C in the absence of B1 for 30 h. The cells were harvested, and native ChIP experiments without cross-linking were performed essentially as described (10). For each experiment, the percentage DNA recovery of ChIP samples relative to the DNA amount in the input was averaged over triplicate quantitative

PCR measurements (Chromo4, Bio-Rad). Primer sequences for *cnt2* (centromeric inner repeats of Chromosome 2), *telo2R* (subtelomeres of Chromosome 2), *mes1* (upstream of *mes1* on Chromosome 1), and *rDNA2* (rDNA) have been published (25, 26). The data represent the average DNA recovery compared with the input DNA samples with standard variances from three replicates. Student's *t* tests were performed between wild type and the indicated strains. The *p* value < 0.05 is denoted with one asterisk (\*) and < 0.01 with two asterisks (\*\*).

**Western Blotting**—To assay total levels of sumoylated proteins, cells were harvested in the appropriate media/conditions and lysed in denaturing buffer (8 M urea, 50 mM NaH<sub>2</sub>PO<sub>4</sub>, 50 mM Tris, pH 8, 300 mM NaCl, 20 mM *N*-ethylmaleimide, 2 mM PMSF, and Complete protease inhibitor EDTA-free). Equal quantities of protein were then resolved on 4–20% gradient Tris-glycine gels and immunoblotted using antisera raised against *S. pombe* SUMO (9). Anti-tubulin was used as a loading control (Sigma). Membranes were then probed with IRDye800 or IRDye680 secondary antibodies (LI-COR Biosciences), and fluorescence was detected using the ODYSSEY Infrared Imaging system (LI-COR 117 Biosciences).

**Mass Spectrometry Analyses**—Samples were denatured and then reduced and alkylated prior to overnight digestion with trypsin. The protein digests were loaded onto MudPIT columns that were placed inline with a 1200 quaternary HPLC pump (Agilent Technologies) and the eluted peptides were electrosprayed directly into an LTQ Orbitrap XL mass spectrometer (Thermo Scientific) using a 10-step MudPIT method. MS/MS spectra were extracted using RawXtract (version 1.9.9) (27). MS/MS spectra were searched with the Sequest algorithm (28) against a *S. pombe* database concatenated to a decoy database in which the sequence for each entry in the original database was reversed (29). Sequest results were assembled and filtered using the DTASelect (version 2.0) algorithm (30).

**In Vitro Pulldown Experiments**—The *S. pombe* SUMO chains were produced as described above. GST-tagged Ufd1 or Ufd1<sup>AAA</sup> were expressed in BL21 cells and purified using glutathione (GSH)-Sepharose (GE Healthcare). Purified SUMO chains and GST-Ufd1 or GST-Ufd1<sup>AAA</sup> were combined in buffer containing 50 mM Tris, pH 8, 150 mM NaCl, 0.5 mM EDTA, 5 mM β-mercaptoethanol at 25 °C for 15 min prior to pulldown with GSH-Sepharose. After extensive washes with the binding buffer, proteins were eluted with 20 mM reduced GSH and analyzed by Western blotting.

## RESULTS

**Ufd1 C-terminal SIM Mediates Non-covalent Interaction between Cdc48-UN Complex and SUMO**—We carried out a proteomic screen to identify SUMO binding proteins that may be involved in STUbL function. Immobilized SUMO chains (or control GST) were used to pull down proteins in cell lysates prepared from fission yeast lacking endogenous SUMO (SUMOΔ). Bound proteins were eluted using purified monomeric SUMO (Fig. 1A), and identified by mass spectrometry. Notably, the fission yeast orthologues of a number of known SUMO interactors were identified in the eluate from the SUMO chain but not the GST column (see supplemental Table S1). Among the SUMO-specific interactors, the Cdc48/p97

## Cooperative Functions of STUbL and Cdc48-Ufd1-Npl4

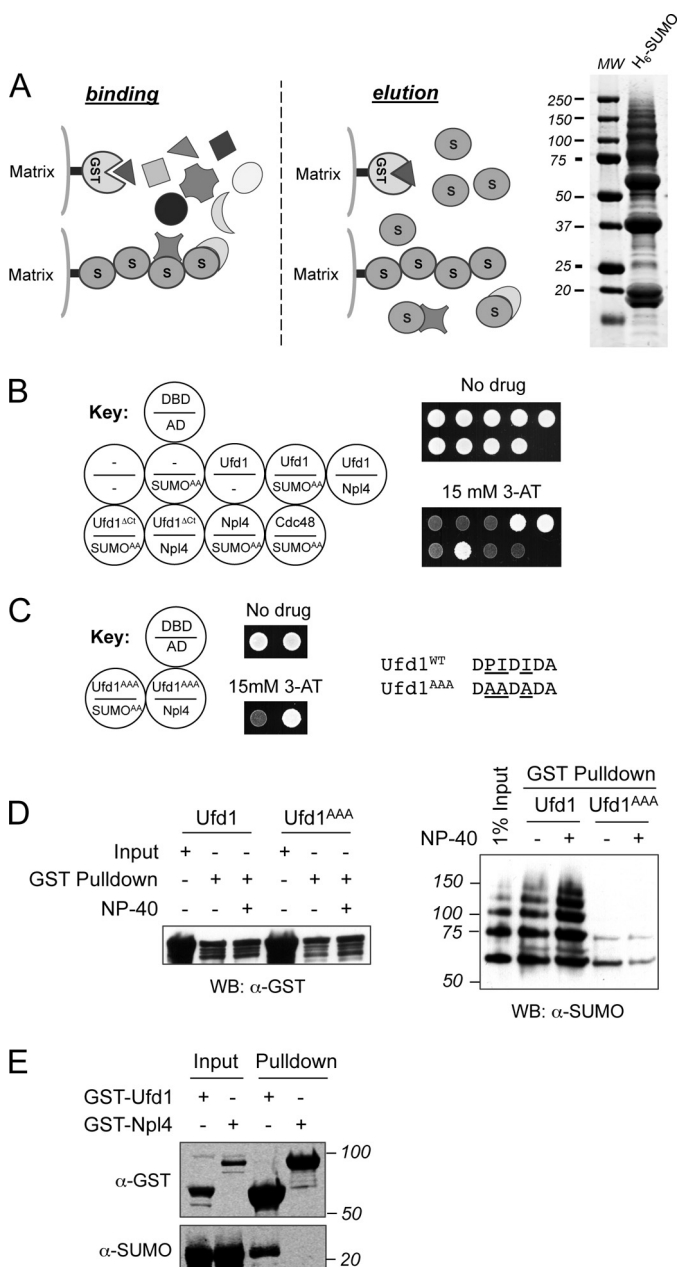


**FIGURE 1. Ufd1 interacts with SUMO *in vivo* via a C-terminal SIM.** *A*, schematics of SUMO chain pull down of *S. pombe* proteins. *S*, SUMO. Cell lysate of a *SUMO* $\Delta$  strain was applied to AffiGel agarose matrix conjugated with SUMO chains or control GST. After binding and washing, bound proteins were eluted by competition with monomeric SUMO. SUMO chains purified from *E. coli* BL21(DE3) expressing the *S. pombe* SUMO pathway were resolved using SDS-PAGE and visualized by Coomassie staining (*right panel*). *B* and *C*, the indicated yeast two-hybrid strains were spotted onto selective plates to identify interacting proteins. The key indicates genes placed in frame with the Gal4 DNA-binding (DBD) or the Gal4-activating domains (AD). *D*, Western analysis using antibodies for GST or SUMO following *in vitro* GSH-Sepharose pull-downs of GST-Ufd1 or GST-Ufd1<sup>AAA</sup> incubated with SUMO chains. All of the above proteins were expressed and purified from *E. coli*. *E*, Western analysis (WB) of GSH-Sepharose pull-downs from lysates of DE3 strains co-expressing His<sub>6</sub>-SUMO with either GST-Ufd1, or GST-Npl4. Immunoblots were probed with antibodies for GST or SUMO. MW, molecular weight.

cofactors Ufd1 and Npl4 were the most highly represented, with ~60% of their primary sequence covered by numerous independent peptides (see supplemental Table S1). This was intriguing, as the Ufd1-Npl4 heterodimer is well characterized

and reported to bind ubiquitylated proteins (31). Nevertheless, we identified a potential SUMO interaction motif (SIM) in the last seven amino acids (DPIDIDA) of Ufd1, which deviates somewhat from the core consensus I/V-X-I/V-I/V or I/V-I/V-X-I/V sequence, but closely resembles the SIM found in the SUMO-2 binding protein CoREST1 (NPIDIEV; (32)). Notably, the budding yeast Ufd1 protein also terminates with a SIM-containing sequence (EYIEID), which matches the core consensus motif I/V-I/V-X-I/V. Consistently, budding yeast Ufd1 was identified as a SUMO interactor in recent high throughput yeast two-hybrid analyses (33, 34). In the latter study, all Ufd1 clones identified encoded the C terminus of the protein but lacked various extents of the N terminus, indicating that the SUMO interaction site resides in the C terminus of Ufd1. However, neither the function nor the nature of the interaction (covalent *versus* non-covalent, direct *versus* indirect) was defined in those studies. Therefore, we tested for non-covalent interaction between Cdc48-UN and a non-conjugatable form of SUMO (SUMO<sup>AAA</sup>) using pairwise yeast two-hybrid analyses. We determined that Ufd1 but neither Npl4 nor Cdc48 interacted with SUMO (Fig. 1B); and confirmed the known interaction between Ufd1 and Npl4 (35). Removing the putative SIM, by deleting the last seven amino acids of the unstructured C terminus (Ufd1<sup>ΔCt</sup>) of Ufd1 abolished interaction with SUMO but did not affect the interaction between Ufd1 and Npl4 (Fig. 1B). Furthermore, mutating the hydrophobic residues in the Ufd1 C-terminal SIM to alanine (DAADADA; Ufd1<sup>AAA</sup>) also abolished the interaction of Ufd1 with SUMO but not with Npl4 (Fig. 1C).

To confirm that Ufd1 interacts directly and non-covalently with SUMO, we expressed and purified GST-Ufd1, GST-Ufd1<sup>AAA</sup>, and His<sub>6</sub>-SUMO chains from bacteria and tested their interactions *in vitro*. Compared with GST-Ufd1, which bound SUMO robustly, GST-Ufd1<sup>AAA</sup> showed only background levels of SUMO binding (Fig. 1D), consistent with our yeast two-hybrid analyses and proteomic approaches. Therefore, Ufd1 contains a *bona fide* C-terminal SIM that mediates direct and non-covalent interaction with SUMO *in vitro*. As anticipated for a protein that contains a single SIM and not the tandem arrangements observed in STUbL proteins (36), we did not observe preferential binding of Ufd1 to the higher molecular weight SUMO chain species.

We further confirmed that GST-Ufd1, but not GST-Npl4, interacts directly with SUMO (Fig. 1E). Taken together, our analyses thus far indicate that Cdc48-UN interacts non-covalently with SUMO via a SIM in Ufd1, which is conserved in the two distantly related fission and budding yeasts.

**Colocalization of Ufd1 with SUMO *in Vivo***—We next tested the interaction of Ufd1 with SUMO chains *in vivo*. We previously showed that upon inactivation of the STUbL Slx8-Rfp1, SUMO chains accumulate to high levels, as detected by Western blotting (9, 37). Similarly, here we found that GFP-SUMO forms one to two nuclear foci in *slx8-29* temperature-sensitive cells, and both the frequency and size of these foci dramatically increased upon a shift from permissive (25 °C) to restrictive temperature (35 °C; Fig. 2A). These foci represent an accumulation of localized SUMO chains, as when all (SUMO<sup>K0</sup>) or major (SUMO<sup>K14R,K30R</sup>) SUMO acceptor lysines were mutated



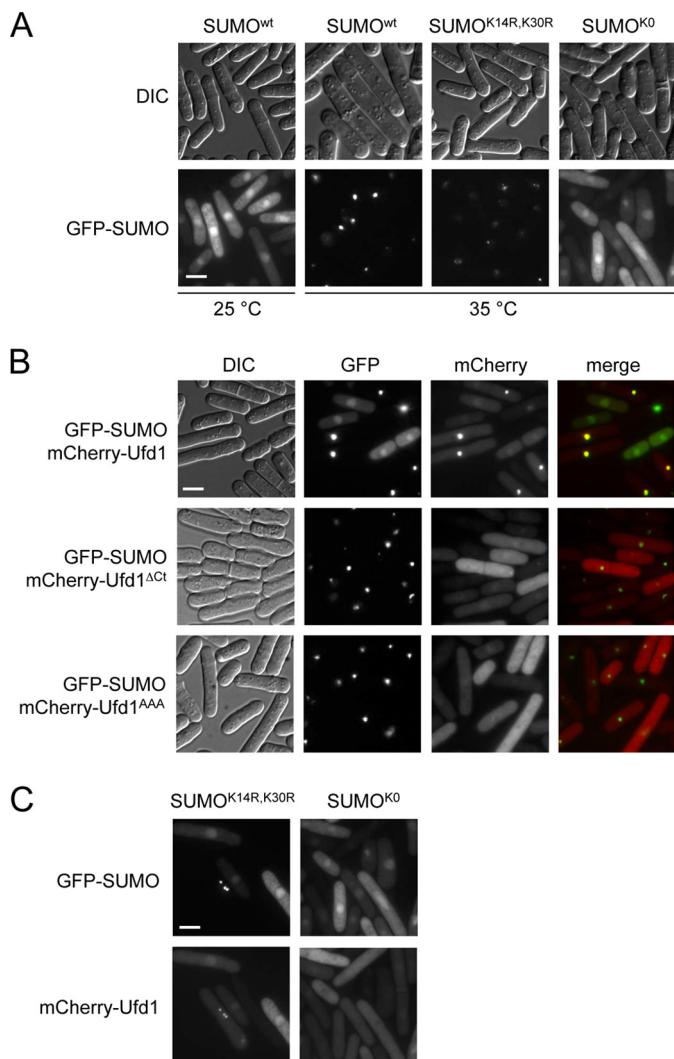


FIGURE 2. *A*, fluorescence imaging of live *slx8-29* cells, expressing GFP fusions of SUMO<sup>WT</sup>, SUMO<sup>K14R,K30R</sup>, or SUMO<sup>K0</sup> from the *nmt41* promoter and inactivated at 35 °C for 6 h. *Bar*, 5  $\mu$ m. *DIC*, differential interference contrast. *B*, GFP-SUMO and mCherry-Ufd1 (wild type, Ufd1 <sup>$\Delta$ Ct</sup>, or Ufd1<sup>AAA</sup> mutant) were co-expressed in *slx8-29* cells, which were inactivated at 35 °C for 6 h. The mCherry-Ufd1 and SUMO constructs were expressed using the *nmt41* and the *nmt42* promoters, respectively. Cells were cultured in the absence of thiamine (B1) at 25 °C for 2 days and then inactivated at 35 °C for 6 h before live cell imaging. *Bar*, 5  $\mu$ m. *C*, live cell imaging of *slx8-29* mutants, co-expressing either GFP-SUMO<sup>K14R,K30R</sup> or SUMO<sup>K0</sup> with mCherry-Ufd1. *Bar*, 5  $\mu$ m.

to arginine, these foci were either not observed or were greatly diminished, respectively (Fig. 2A) (9). Strikingly, mCherry-Ufd1 also formed intense foci in *slx8-29* cells at restrictive temperature, which tightly colocalized with the GFP-SUMO foci (Fig. 2B).

Underscoring our biochemical and genetic data, deletion or mutation of the Ufd1 SIM completely abrogated the formation of Ufd1 foci, and colocalization with SUMO (Fig. 2B; Ufd1 <sup>$\Delta$ Ct</sup> Ufd1<sup>AAA</sup>). Furthermore, in *slx8-29* cells expressing GFP-SUMO<sup>K0</sup>, which is unable to form chains or foci, the mCherry-Ufd1 signal remained diffuse (Fig. 2C). However, in GFP-SUMO<sup>K14R,K30R</sup> expressing *slx8-29* cells, mCherry-Ufd1 again formed foci that both colocalized with (Fig. 2C) and matched the reduced size of SUMO foci in this background (see Fig. 2A). This result also indicates that Ufd1 does not require a specific

SUMO chain topology, as alternative acceptor sites are used to form the limited chains in the SUMO<sup>K14R,K30R</sup> background (9). Indeed, as alluded to above, we believe that the single SIM present in Ufd1 is unlikely to favor binding of the protein to SUMO chains over monomeric SUMO. However, SUMO chains could potentially provide binding sites for multiple Ufd1 proteins. Overall, we have demonstrated that Ufd1 interacts with SUMO non-covalently and that it colocalizes with SUMO *in vivo*, in a SIM-dependent manner.

*Ufd1 Is Important for Maintaining Genome Stability*—STUbl mutants exhibit genome instability and are hypersensitive to genotoxins, due to defects in SUMO-dependent protein regulation (9). As Ufd1 physically and may also functionally intersect with the SUMO pathway, we tested whether hypomorphic Ufd1 mutants were also sensitive to DNA damaging agents. Ufd1 is essential for viability, so we generated a number of temperature-sensitive alleles that were expressed from the endogenous *ufd1* locus (Fig. 3A). All except one of the eight *ufd1 ts* alleles we identified contain point mutations within the conserved UFD1 domain. Western blot analysis revealed that the *ufd1-1* allele, which was used in subsequent experiments, became destabilized upon shifting of temperature from permissive (25 °C) to non-permissive (35 °C) conditions (data not shown). As expected, the growth of the majority of Ufd1 mutant strains was strongly inhibited at restrictive temperature (Fig. 3B). At semi-permissive temperature, Ufd1 mutants were hypersensitive to a number of genotoxins, including the replication inhibitor hydroxyurea, the alkylating agent methyl methanesulfonate, and the topoisomerase I poison camptothecin (Fig. 3B). Therefore, similar to STUbl, fission yeast Ufd1 plays a key role in cell survival following genotoxic stress.

*Ufd1 Is Involved in SUMO Chain Metabolism*—The known roles of Cdc48-UN in proteolysis, together with our findings that it interacts with SUMO and is required for cellular resistance to DNA damaging agents, suggested to us that the complex might have a previously undefined role in SUMO pathway homeostasis. Therefore, we assayed SUMO chain formation in Ufd1 mutants *in vivo*, using the foregoing GFP-SUMO foci reporter system (see Fig. 2A). Notably, *ufd1-1* mutant cells, similar to *slx8-29*, also accumulated GFP-SUMO foci, although they were not as numerous or bright as those in *slx8-29* cells (Fig. 4, A and B). Double mutant *slx8-29 ufd1-1* cells accumulated GFP-SUMO foci that were qualitatively similar to those in *slx8-29* cells (Fig. 4, A and B). Interestingly, GFP-SUMO foci were not detected in an *mts3-1* proteasome mutant (Fig. 4A). This indicates that when Slx8 or Ufd1 are still functional, they can counteract focal SUMO chain accumulation, independently of proteasomal activity.

We extended our analysis to determine the effects of Ufd1 inactivation on total cellular SUMO conjugates, as detected by Western analysis. Compared with wild type, *slx8-29* cells accumulated sumoylated species that were especially evident in the higher molecular weight range (Fig. 4C) (4, 9, 37). Consistent with our GFP-SUMO foci data, *ufd1-1* cells also accumulated higher molecular weight SUMO conjugates, albeit to a lesser degree, and *ufd1-1 slx8-29* double mutants exhibited an increase in these conjugates over the *slx8-29* single mutant, whereas the *mts3-1* proteasome mutant predominantly accu-

## Cooperative Functions of STUbL and Cdc48-Ufd1-Npl4

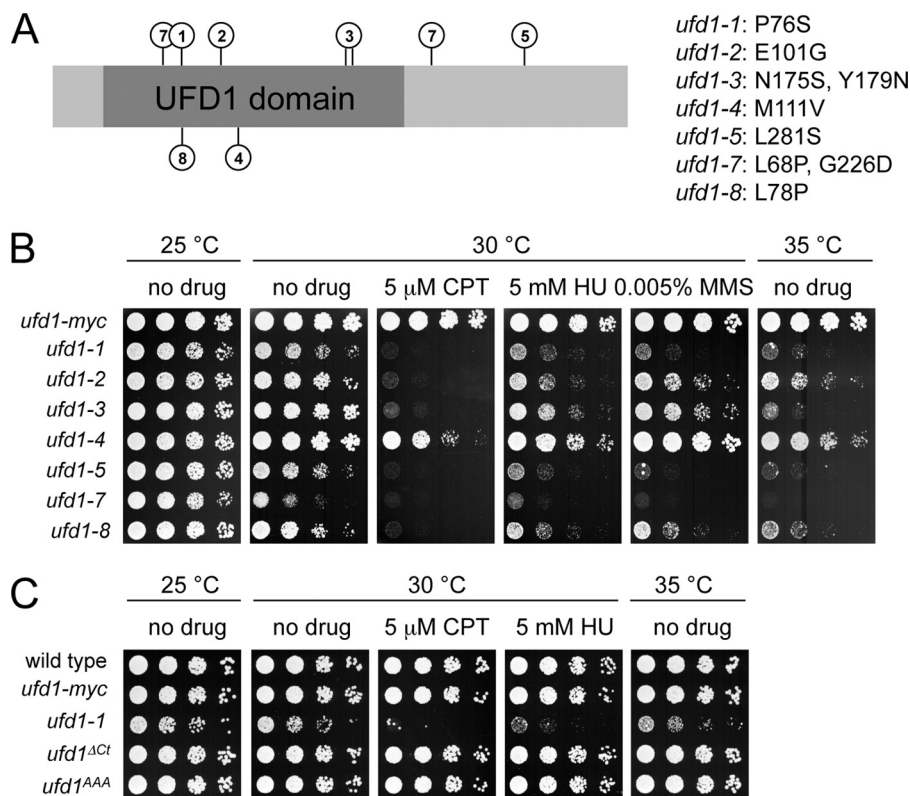


FIGURE 3. *A*, graphic representation of the point mutations within the *ufd1* temperature-sensitive mutants. The amino acid changes within each mutant are also shown on the right. *B* and *C*, serial dilutions of the indicated strains were spotted onto media with or without genotoxins and grown at the indicated temperatures. *HU*, hydroxyurea; *CPT*, camptothecin; *MMS*, methyl methanesulfonate.

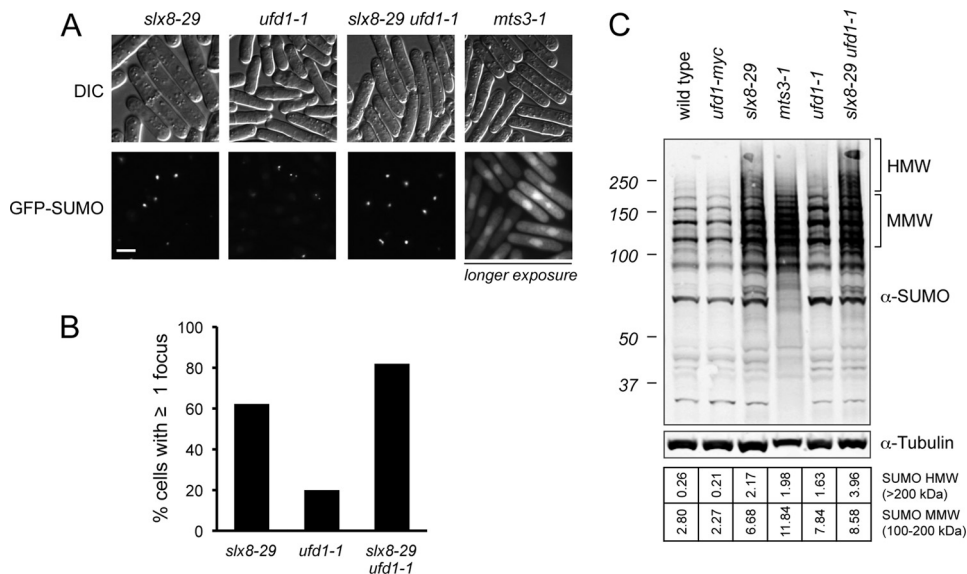
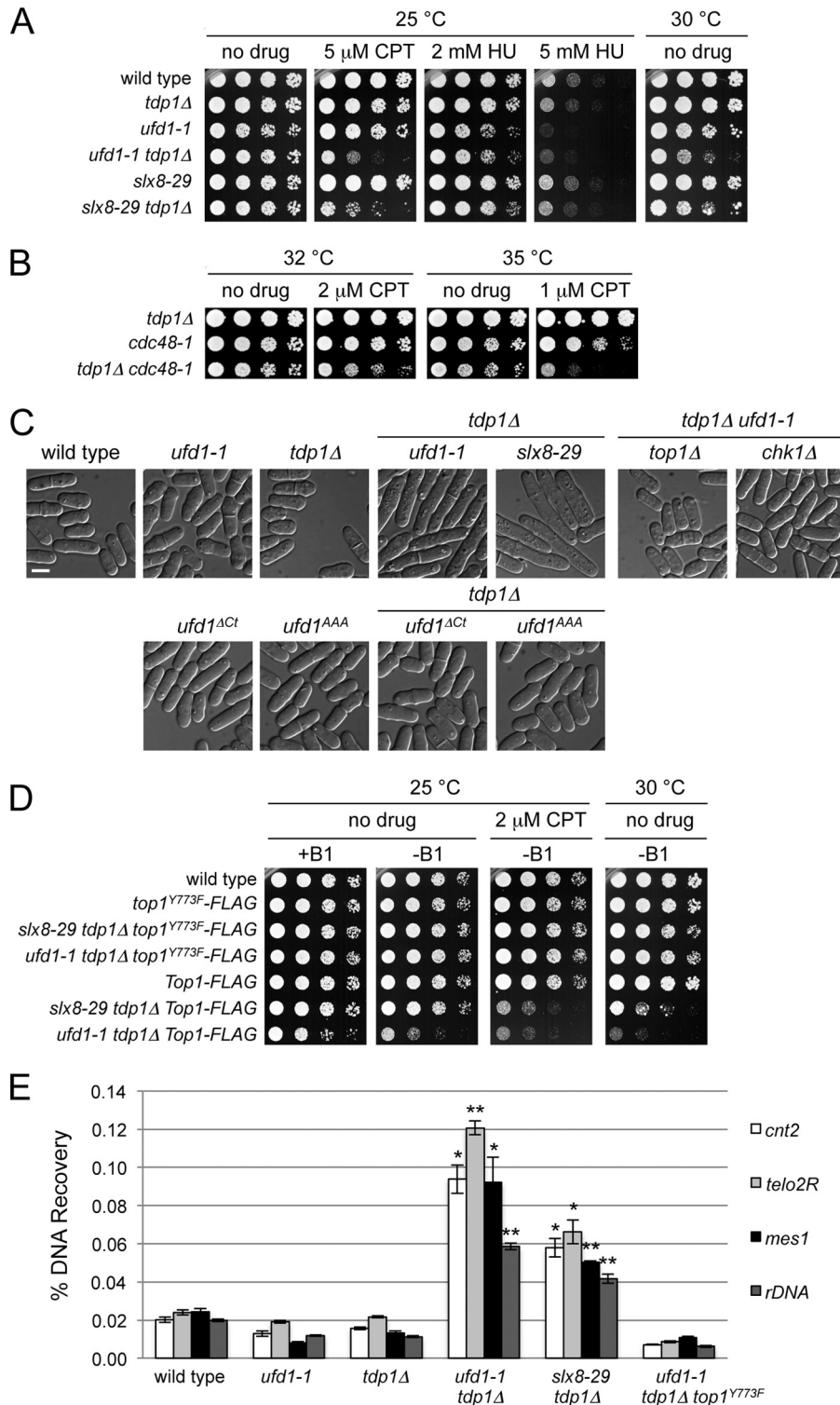


FIGURE 4. **Ufd1 antagonizes SUMO chain accumulation.** *A*, GFP-SUMO was expressed as described in Fig. 2*A* in the indicated strains, which were inactivated at 35 °C for 6 h before imaging. Bar, 5 μm. *DIC*, differential interference contrast. *B*, graph depicting percentage of cells with one or more GFP-SUMO foci observed in the indicated mutant. At least 250 cells were scored for each strain. *C*, total levels of sumoylated proteins. Indicated strains were cultured at 25 °C to mid log phase then shifted to 35 °C for 8 h. SUMO protein levels were quantitated and normalized against tubulin using the ODYSSEY Infrared Imaging system (LI-COR Biosciences). *HMW*, high molecular weight; *MMW*, medium molecular weight.

mutated medium molecular weight range SUMO conjugates, which were not prone to accumulate in visible nuclear foci (Fig. 4, *A* and *C*).

**Cdc48-UN Function Is Critical in Absence of DNA Repair Enzyme Tdp1**—We recently identified a potent and evolutionarily conserved negative genetic interaction between Slx8

(STUbL) mutants and a deletion of tyrosyl DNA phosphodiesterase (Tdp1 (10, 38)). As our analyses have implicated Cdc48-UN in SUMO and STUbL-related genome stability functions, we determined the phenotype of *ufd1-1 tdp1Δ* double mutant cells. Strikingly, similar to *slx8-29 tdp1Δ*, *ufd1-1 tdp1Δ* double mutant cells were extremely elongated, slow



**FIGURE 5. When combined with *tdp1Δ* cells, the *Cdc48*-UN complex mutants were synergistically sensitive to camptothecin and have increased levels of spontaneous Top1cc.** *A*, *B*, and *D*, serial dilutions of the indicated strains were spotted onto media with or without genotoxins. *C*, cells of the indicated genotypes were cultured in liquid media at 25 °C to mid-log phase and imaged with a Nikon Eclipse E800 microscope. Bar, 5 μm. *E*, native ChIP-quantitative PCR assays of an *mtt1*-inducible FLAG-Top1 integrated at Top1 endogenous locus in the indicated strains. Student's *t* tests were performed between wild type and the indicated strains. Error bars show S.D. \*, *p* value < 0.05; \*\*, *p* value < 0.01. HU, hydroxyurea; CPT, camptothecin.

growing, and more sensitive to genotoxins when compared with either single mutant (Fig. 5, *A* and *C*). This phenotype was completely reversed by deleting Top1 (Fig. 5*C*), echoing the identical rescue of *slx8-29 tdp1Δ* synthetic sickness by Top1 deletion (10). The elongated phenotype of *ufd1-1 tdp1Δ* cells is

due to activation of the DNA damage checkpoint kinase Chk1, which blocks cell cycle progression by antagonizing CDK activation (10, 39). Consistently, *ufd1-1 tdp1Δ chk1Δ* triple mutant cells were not elongated (Fig. 5*C*). Although it is well established that Ufd1 functions with Cdc48, we wished to confirm



that the genetic interaction between *ufd1-1* and *tdp1Δ* was also observed between a Cdc48 hypomorph and *tdp1Δ*. To this end, we generated a temperature-sensitive Cdc48 allele (*cdc48-1*), from which we created a *cdc48-1 tdp1Δ* double mutant, and compared its growth at 32 and 35 °C to that of the single mutants, in the presence and absence of camptothecin. As for *ufd1-1*, we observed synergistic camptothecin sensitivity of the *cdc48-1 tdp1Δ* strain compared with that observed in either single mutant (Fig. 5B). Again, in the absence of camptothecin, *cdc48-1 tdp1Δ* cells exhibited the highly elongated phenotype characteristic of *ufd1-1 tdp1Δ* or *slx8-29 tdp1Δ* double mutants (data not shown). These data are consistent with the concerted action of the Cdc48-UN complex in protecting genome stability against spontaneous Top1 lesions in the absence of Tdp1, strikingly mirroring our findings for STUbL mutants.

**Elevated Levels of Spontaneous Top1cc in *ufd1-1 tdp1Δ* Cells**—We previously showed that elevated levels of stalled covalent Top1-DNA adducts, also known as Top1 cleavage complexes (Top1cc) cause the severe growth and genome instability phenotypes of *slx8-29 tdp1Δ* cells (10). As deleting Top1 reverses the *ufd1-1 tdp1Δ* phenotype, we tested whether there were increased levels of Top1cc in this background as well, which would account for activation of the G<sub>2</sub> DNA damage checkpoint in cells lacking Tdp1 (10). We initially determined the effects of expressing wild type Top1 versus the active site mutant Top1<sup>Y773F</sup> in *ufd1-1 tdp1Δ* cells and other selected genetic backgrounds. Wild type Top1 was highly toxic to both *ufd1-1 tdp1Δ* and *slx8-29 tdp1Δ* cells in the presence of camptothecin, whereas Top1<sup>Y773F</sup> had no deleterious effect on the growth of either strain (Fig. 5D). Strikingly, even in the absence of camptothecin, wild type Top1 at both permissive and semi-permissive temperatures strongly inhibits the growth of the *ufd1-1 tdp1Δ* double mutant (Fig. 5D). Therefore, Top1 catalytic activity and hence its ability to form Top1cc causes toxicity in *ufd1-1 tdp1Δ* cells.

To quantify Top1cc levels, we performed a modified native chromatin immunoprecipitation and quantitative PCR assay (10) to examine covalent chromatin association of Top1. Similar basal levels of Top1cc were observed in wild type, *ufd1-1*, and *tdp1Δ* single mutant cells (Fig. 5E). However, in the *ufd1-1 tdp1Δ* double mutant, there was a significant increase in Top1cc at all four loci analyzed (Fig. 5E). The increase in Top1cc in *ufd1-1 tdp1Δ* cells was similar to that seen in *slx8-29 tdp1Δ* cells (10) and was abolished in the Top1<sup>Y773F</sup> catalytic mutant (Fig. 5E). Comparable levels of Top1 expression in each background were verified via Western analysis (data not shown). Thus, as suggested by our genetic analyses, there is an increase in stable spontaneous Top1cc in *ufd1-1 tdp1Δ* mutants, which accounts for the genomic instability of these cells.

**Critical Role of Ufd1 C-terminal SIM when STUbL Function Is Compromised**—Our data demonstrate that the Cdc48-UN complex can interact with SUMO via a C-terminal SIM in Ufd1 and that both Ufd1 and STUbL share a role in suppressing Top1cc-induced genome instability. To gain further insight into the physiological function of the interaction between Ufd1 and SUMO, we replaced the endogenous Ufd1 gene with one that encodes Ufd1 lacking its C-terminal SIM (Ufd1<sup>ΔCt</sup>; see Fig.

1B). Cells expressing Ufd1<sup>ΔCt</sup> were indistinguishable from wild type either at high temperature or in the presence of genotoxins (Fig. 6A, Fig. 3C, and Fig. 5C). In addition, Ufd1<sup>ΔCt</sup> cells deleted for Tdp1 did not show enhanced camptothecin sensitivity over *tdp1Δ* cells (Fig. 6A). Therefore, we hypothesized that the Ufd1-SUMO interaction might be partly redundant with other recruitment signals used by Cdc48-UN such as ubiquitylation. As both STUbL and the Cdc48-UN complex cooperate in a Top1cc repair pathway parallel to Tdp1, we tested for genetic interaction between Ufd1<sup>ΔCt</sup> and *slx8-29*, in the presence or absence of Tdp1. We performed tetrad dissections on asci produced from a genetic cross between *slx8-29 ufd1<sup>ΔCt</sup>* and *tdp1Δ* cells. Fission yeast meiosis produces four haploid spores, which can be micromanipulated prior to germination to allow analysis of each resultant genotype. Such analysis determines whether a particular genotype has defects in germination and subsequent propagation, which is indicative of a genetic interaction. Strikingly, the *slx8-29 tdp1Δ* phenotype was strongly exacerbated by the Ufd1<sup>ΔCt</sup> mutation (Fig. 6B). Indeed, unlike *slx8-29 tdp1Δ*, the *slx8-29 tdp1Δ ufd1<sup>ΔCt</sup>* triple mutant cells could not be further propagated following tetrad dissection, due to extreme sickness. This synthetic phenotype was not caused by the presence of an epitope tag on Ufd1, as *ufd1-myc* showed no genetic interaction in the *slx8-29 tdp1Δ* background (Fig. 6C). We also tested whether *ufd1* SIM mutants (*ufd1<sup>ΔCt</sup>* or *ufd1<sup>AAA</sup>*) had a more general role in cell growth when SUMO conjugates accumulated in a hypo-ubiquitylated state in *slx8-29* cells at elevated temperatures. The growth of *slx8-29* cells was further compromised at permissive and semi-permissive temperatures by the presence of Ufd1<sup>ΔCt</sup> or Ufd1<sup>AAA</sup> and was strongly defective at restrictive temperature, versus *slx8-29* cells alone (Fig. 6D). Thus, when STUbL activity is compromised and SUMO conjugates are not (or not extensively) ubiquitylated, the ability of Ufd1 to bind SUMO becomes critical. Such redundancy in cell signaling is a recurrent and important theme as discussed below. The synthetic sickness between *slx8-29* and *ufd1* SIM mutants was fully rescued by reducing the ability of SUMO to form chains (SUMO<sup>K14R,K30R</sup>; Fig. 6D), indicating that the essential functions of Slx8 and Ufd1 converge on reducing or eliminating the toxic higher molecular weight SUMO chain species in a cell.

## DISCUSSION

Herein, we reveal and functionally define a non-covalent interaction between the Cdc48-UN complex and SUMO mediated by a SIM at the Ufd1 C terminus. The known interaction with ubiquitin of the Cdc48-UN complex (40), together with its novel ability to interact with SUMO, make Cdc48-UN an excellent candidate as a STUbL cofactor, working either alongside or downstream of STUbL. Our genetic analysis certainly supports a cooperative function for fission yeast STUbL and the Cdc48-UN complex in mitigating the genome destabilizing effects of Top1cc and also indicates a broader concerted action in other as yet unidentified DNA repair processes. Given the conservation of the SUMO interaction and SIM in the distantly related budding yeast Ufd1 (Refs. 33, 34, and this study), the cooperation between STUbL and Cdc48-UN is likely to be broadly conserved in eukaryotes. Intriguingly, in this regard,

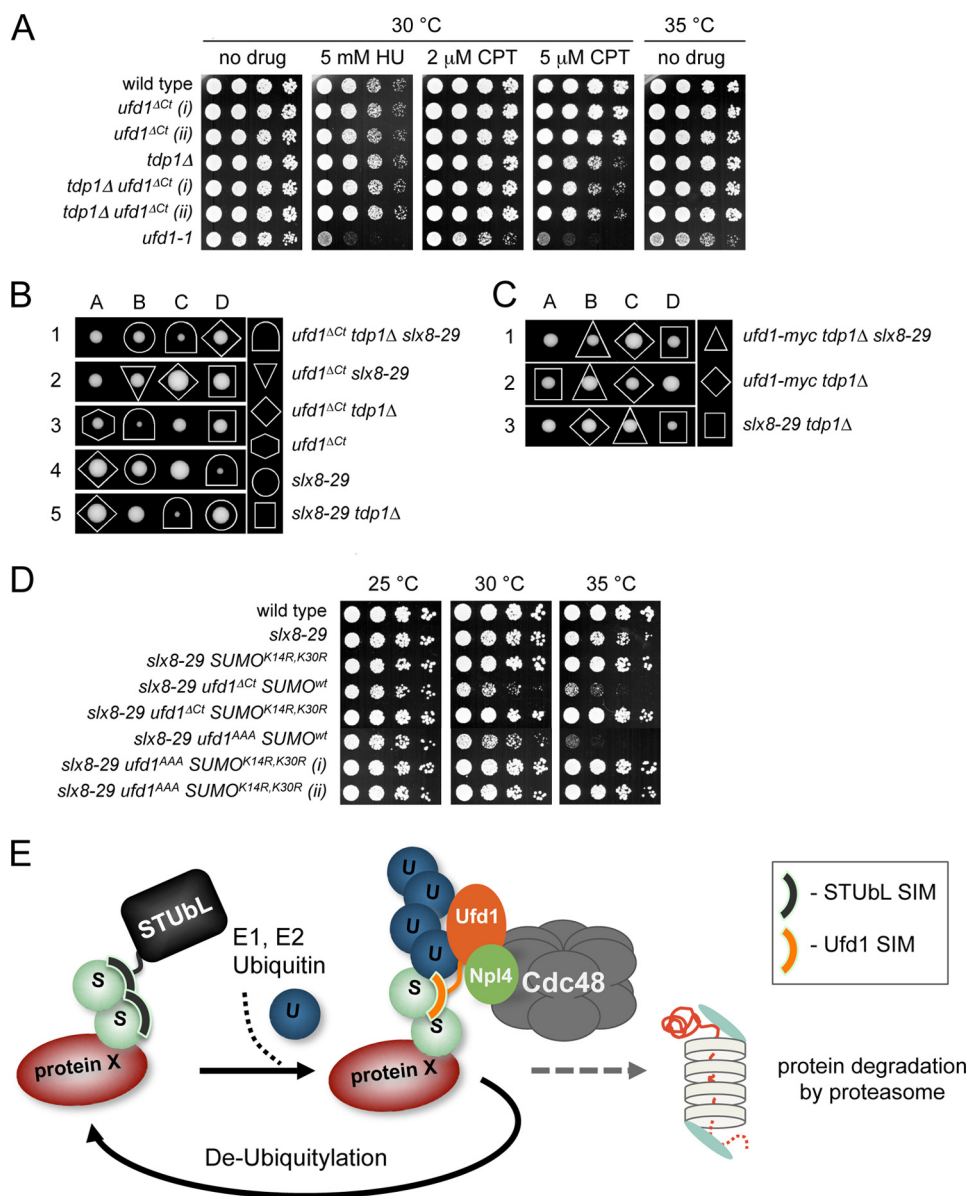


**FIGURE 6. Critical role of Ufd1 C-terminal SIM when STUbL function is compromised.** *A* and *D*, serial dilutions of the indicated strains were spotted onto media and grown at the indicated temperatures. *B* and *C*, representative tetrad dissections are shown from a genetic cross between *slx8-29* cells and *tdp1Δ ufd1<sup>ΔCt</sup>* (*B*) or *tdp1Δ ufd1-myc* (*C*) strains. The key depicts the genotype of each spore. Wild type cells are unlabeled. *E*, model for Cdc48-UN targeting through the novel dual recognition of ubiquitin and SUMO. See text for further details. *HU*, hydroxyurea; *CPT*, camptothecin; *U*, ubiquitin; *S*, SUMO.

budding yeast Cdc48-UN was recently shown to remove ubiquitinated Mat  $\alpha$ 2 transcription factor from its promoter sites (41). Budding yeast STUbL is in part responsible for the ubiquitylation of Mat  $\alpha$ 2 and executes this role in a SIM-dependent manner (41, 42). Thus, although as yet untested, budding yeast Cdc48-UN may also recognize Mat  $\alpha$ 2 through ubiquitin and SUMO binding motifs.

As is often the case with SIM motifs, we do not observe a clear SIM in the same location in the human Ufd1 C terminus. For example, we identified SIMs in distinct positions and number in different species when we initially defined the STUbL family (36). Nevertheless, they all exhibit SUMO interaction and share the same mechanism of action. Furthermore, the UvrD family helicase of budding yeast, Srs2, contains a SIM at its C terminus, which recruits it to SUMO-modified proliferating cell nuclear antigen (43). This was long thought to be a budding yeast spe-

cific phenomenon, given the lack of a conserved SIM in the fission yeast Srs2 C terminus or a clear human Srs2 ortholog. However, it turns out that a SIM located in the middle of the human UvrD-like helicase called PARI likely recruits it to SUMO-modified proliferating cell nuclear antigen to execute Srs2-like functions (44).

DNA repair processes in budding yeast, *Caenorhabditis elegans*, and mammalian cells were only recently shown to critically depend on the Cdc48-UN complex (14, 16–18). Human Cdc48/p97 is recruited to DSBs by Ufd1-Npl4 and Lys-48-linked ubiquitin. Cdc48/p97 promotes the turnover of Lys-48-linked ubiquitin conjugates at DNA damage sites and is important for the proper association of critical DNA repair factors such as 53BP1, BRCA1, and Rad51 with DSB sites (18). Cdc48/p97-mediated targeting of 53BP1 to DSBs has been attributed to its role in displacing polycomb group protein L3MBTL1,



which binds the same H4-K20me2 modification as 53BP1 (17). Furthermore, Cdc48/p97 and Ufd1 mediate the UV-induced turnover of RNA polymerase II and the replication-licensing factor CDT1 (14, 16). A unifying theme in these Cdc48/p97 functions appears to be the stripping or disassembly of ubiquitylated substrates from large protein complexes, or its so-called segregase activity. This segregase function may not always be coupled to protein degradation, as there is evidence for deubiquitylation of proteins once evicted from a protein complex (12), which could provide for rapidly reversible “toggling” of protein activity. In this regard, it is interesting to note that either STUbL or Cdc48-UN dysfunction causes SUMO chains to accumulate in subnuclear foci, whereas proteasomal inhibition does not. We propose that this is a result of concerted STUbL and Cdc48-UN-mediated “extraction” of SUMO conjugates from chromatin (similar to Mat  $\alpha$ 2; (41, 42)), and/or regulation of the SUMO pathway enzymes, which can inhibit SUMO chain formation, independent of proteasomal turnover.

Our discovery that Ufd1 can bind not only to ubiquitin but also with SUMO has important ramifications for Cdc48-UN function and may hint at a more pervasive mechanism in “reading” these posttranslational modifications (Fig. 6E). Through Ufd1, Cdc48-UN could be recruited to a subset of proteins that are co-modified with SUMO and ubiquitin, such as STUbL targets (36). The recognition of STUbL substrates by Cdc48-UN could either facilitate the degradation of these proteins by the proteasome or their de-ubiquitylation (and possibly de-sumoylation) and recycling back to a functional pool (Fig. 6E). Such dual recognition of ubiquitin and SUMO may provide additional flexibility, cooperativity, and specificity to substrate targeting, as exemplified by the recent characterization of tandem PCNA Interacting Protein (PIP)-SIM receptor motifs in Srs2 for the recognition of sumoylated proliferating cell nuclear antigen (45). Cooperative recognition of distinct protein modifications is an emerging mechanism in the regulation of cellular activities such as DNA damage repair. For example, Crb2, an *S. pombe* ortholog of metazoan 53BP1, recognizes both H2A phosphorylation and H4-K20 methylation to promote the optimal accumulation of Crb2 at DNA damage sites (46, 47). In addition to phosphorylation and ubiquitylation, sumoylation of DNA repair factors also occurs on a large scale upon DNA damage (48–50). Therefore, the ubiquitylation of sumoylated proteins by STUbL may promote their recognition and removal from DSBs or damage sites by the Cdc48-UN complex, thereby critically orchestrating the DNA damage response.

*Acknowledgments*—We thank E. Chang for providing yeast strains and the cell cycle group at TSRI for helpful discussions.

## REFERENCES

- Bekker-Jensen, S., and Mailand, N. (2011) The ubiquitin- and SUMO-dependent signaling response to DNA double-strand breaks. *FEBS Lett.* **585**, 2914–2919
- Ulrich, H. D. (2012) Ubiquitin and SUMO in DNA repair at a glance. *J. Cell Sci.* **125**, 249–254
- Lallemant-Breitenbach, V., Jeanne, M., Benhenda, S., Nasr, R., Lei, M., Peres, L., Zhou, J., Zhu, J., Raught, B., and de Thé, H. (2008) Arsenic degrades PML or PML-RAR $\alpha$  through a SUMO-triggered RNF4/ubiquitin-mediated pathway. *Nat. Cell Biol.* **10**, 547–555
- Prudden, J., Pebernard, S., Raffa, G., Slavina, D. A., Perry, J. J., Tainer, J. A., McGowan, C. H., and Boddy, M. N. (2007) SUMO-targeted ubiquitin ligases in genome stability. *EMBO J.* **26**, 4089–4101
- Sun, H., Levenson, J. D., and Hunter, T. (2007) Conserved function of RNF4 family proteins in eukaryotes: Targeting a ubiquitin ligase to SUMOylated proteins. *EMBO J.* **26**, 4102–4112
- Tatham, M. H., Geoffroy, M. C., Shen, L., Plechanovova, A., Hattersley, N., Jaffray, E. G., Palvimo, J. J., and Hay, R. T. (2008) RNF4 is a poly-SUMO-specific E3 ubiquitin ligase required for arsenic-induced PML degradation. *Nat. Cell Biol.* **10**, 538–546
- Uzunova, K., Götsche, K., Miteva, M., Weisshaar, S. R., Glanemann, C., Schnellhardt, M., Niessen, M., Scheel, H., Hofmann, K., Johnson, E. S., Praefcke, G. J., and Dohmen, R. J. (2007) Ubiquitin-dependent proteolytic control of SUMO conjugates. *J. Biol. Chem.* **282**, 34167–34175
- Xie, Y., Kerscher, O., Kroetz, M. B., McConchie, H. F., Sung, P., and Hochstrasser, M. (2007) The yeast Hex3/Slx8 heterodimer is a ubiquitin ligase stimulated by substrate sumoylation. *J. Biol. Chem.* **282**, 34176–34184
- Prudden, J., Perry, J. J., Nie, M., Vashisht, A. A., Arvai, A. S., Hitomi, C., Guenther, G., Wohlschlegel, J. A., Tainer, J. A., and Boddy, M. N. (2011) DNA repair and global sumoylation are regulated by distinct Ubc9 non-covalent complexes. *Mol. Cell Biol.* **31**, 2299–2310
- Heideker, J., Prudden, J., Perry, J. J., Tainer, J. A., and Boddy, M. N. (2011) SUMO-targeted ubiquitin ligase, Rad60, and Nse2 SUMO ligase suppress spontaneous Top1-mediated DNA damage and genome instability. *PLoS Genet* **7**, e1001320
- Stolz, A., Hilt, W., Buchberger, A., and Wolf, D. H. (2011) Cdc48: A power machine in protein degradation. *Trends Biochem. Sci.* **36**, 515–523
- Yamanaka, K., Sasagawa, Y., and Ogura, T. (2012) Recent advances in p97/VCP/Cdc48 cellular functions. *Biochim. Biophys. Acta* **1823**, 130–137
- Wolf, D. H., and Stolz, A. (2012) The Cdc48 machine in endoplasmic reticulum associated protein degradation. *Biochim. Biophys. Acta* **1823**, 117–124
- Raman, M., Havens, C. G., Walter, J. C., and Harper, J. W. (2011) A genome-wide screen identifies p97 as an essential regulator of DNA damage-dependent CDT1 destruction. *Mol. Cell* **44**, 72–84
- Ramanathan, H. N., and Ye, Y. (2011) Revoking the cellular license to replicate: Yet another AAA assignment. *Mol. Cell* **44**, 3–4
- Verma, R., Oania, R., Fang, R., Smith, G. T., and Deshaies, R. J. (2011) Cdc48/p97 mediates UV-dependent turnover of RNA Pol II. *Mol. Cell* **41**, 82–92
- Acs, K., Luijsterburg, M. S., Ackermann, L., Salomons, F. A., Hoppe, T., and Dantuma, N. P. (2011) The AAA-ATPase VCP/p97 promotes 53BP1 recruitment by removing L3MBTL1 from DNA double-strand breaks. *Nat. Struct. Mol. Biol.* **18**, 1345–1350
- Meerang, M., Ritz, D., Paliwal, S., Garajova, Z., Bosshard, M., Mailand, N., Jancsak, P., Hübscher, U., Meyer, H., and Ramadan, K. (2011) The ubiquitin-selective segregase VCP/p97 orchestrates the response to DNA double-strand breaks. *Nat. Cell Biol.* **13**, 1376–1382
- Franz, A., Orth, M., Pirson, P. A., Sonnevile, R., Blow, J. J., Gartner, A., Stemmann, O., and Hoppe, T. (2011) CDC-48/p97 coordinates CDT-1 degradation with GINS chromatin dissociation to ensure faithful DNA replication. *Mol. Cell* **44**, 85–96
- Dobrynin, G., Popp, O., Romer, T., Bremer, S., Schmitz, M. H., Gerlich, D. W., and Meyer, H. (2011) Cdc48/p97-Ufd1-Npl4 antagonizes Aurora B during chromosome segregation in HeLa cells. *J. Cell Sci.* **124**, 1571–1580
- Cheng, Y. L., and Chen, R. H. (2010) The AAA-ATPase Cdc48 and cofactor Shp1 promote chromosome bi-orientation by balancing Aurora B activity. *J. Cell Sci.* **123**, 2025–2034
- Meyer, H., Drozdowska, A., and Dobrynin, G. (2010) A role for Cdc48/p97 and Aurora B in controlling chromatin condensation during exit from mitosis. *Biochem. Cell Biol.* **88**, 23–28
- Ramadan, K., Bruderer, R., Spiga, F. M., Popp, O., Baur, T., Gotta, M., and Meyer, H. H. (2007) Cdc48/p97 promotes reformation of the nucleus by extracting the kinase Aurora B from chromatin. *Nature* **450**, 1258–1262
- Moreno, S., Klar, A., and Nurse, P. (1991) Molecular genetic analysis of fission yeast *Schizosaccharomyces pombe*. *Methods Enzymol.* **194**,

- 795–823
25. Hayashi, M., Katou, Y., Itoh, T., Tazumi, A., Tazumi, M., Yamada, Y., Takahashi, T., Nakagawa, T., Shirahige, K., and Masukata, H. (2007) Genome-wide localization of pre-RC sites and identification of replication origins in fission yeast. *EMBO J.* **26**, 1327–1339
  26. Yokobayashi, S., Yamamoto, M., and Watanabe, Y. (2003) Cohesins determine the attachment manner of kinetochores to spindle microtubules at meiosis I in fission yeast. *Mol. Cell Biol.* **23**, 3965–3973
  27. McDonald, W. H., Tabb, D. L., Sadygov, R. G., MacCoss, M. J., Venable, J., Graumann, J., Johnson, J. R., Cociorva, D., and Yates, J. R., 3rd. (2004) MS1, MS2, and SQT—three unified, compact, and easily parsed file formats for the storage of shotgun proteomic spectra and identifications. *Rapid Commun. Mass Spectrom.* **18**, 2162–2168
  28. Eng, J. K., McCormack, A. L., and Yates, J. R., 3rd. (1994) An approach to correlate tandem mass spectral data of peptides with amino acid sequences in a protein database. *J. Am. Soc. Mass Spectrom.* **5**, 976–989
  29. Peng, J., Elias, J. E., Thoreen, C. C., Licklider, L. J., and Gygi, S. P. (2003) Evaluation of multidimensional chromatography coupled with tandem mass spectrometry (LC/LC-MS/MS) for large-scale protein analysis: The yeast proteome. *J. Proteome Res.* **2**, 43–50
  30. Tabb, D. L., McDonald, W. H., and Yates, J. R., 3rd. (2002) DTASelect and Contrast: Tools for assembling and comparing protein identifications from shotgun proteomics. *J. Proteome Res.* **1**, 21–26
  31. Bays, N. W., and Hampton, R. Y. (2002) Cdc48-Ufd1-Npl4: Stuck in the middle with Ub. *Curr. Biol.* **12**, R366–371
  32. Ouyang, J., Shi, Y., Valin, A., Xuan, Y., and Gill, G. (2009) Direct binding of CoREST1 to SUMO-2/3 contributes to gene-specific repression by the LSD1/CoREST1/HDAC complex. *Mol. Cell* **34**, 145–154
  33. Hannich, J. T., Lewis, A., Kroetz, M. B., Li, S. J., Heide, H., Emili, A., and Hochstrasser, M. (2005) Defining the SUMO-modified proteome by multiple approaches in *Saccharomyces cerevisiae*. *J. Biol. Chem.* **280**, 4102–4110
  34. Parnas, O., Amishay, R., Liefshitz, B., Zipin-Roitman, A., and Kupiec, M. (2011) Elg1, the major subunit of an alternative RFC complex, interacts with SUMO-processing proteins. *Cell Cycle* **10**, 2894–2903
  35. Meyer, H. H., Shorter, J. G., Seemann, J., Pappin, D., and Warren, G. (2000) A complex of mammalian ufd1 and npl4 links the AAA-ATPase, p97, to ubiquitin and nuclear transport pathways. *EMBO J.* **19**, 2181–2192
  36. Perry, J. J., Tainer, J. A., and Boddy, M. N. (2008) A SIM-ultaneous role for SUMO and ubiquitin. *Trends Biochem. Sci.* **33**, 201–208
  37. Prudden, J., Perry, J. J., Arvai, A. S., Tainer, J. A., and Boddy, M. N. (2009) Molecular mimicry of SUMO promotes DNA repair. *Nat. Struct. Mol. Biol.* **16**, 509–516
  38. Collins, S. R., Miller, K. M., Maas, N. L., Roguev, A., Fillingham, J., Chu, C. S., Schuldiner, M., Gebbia, M., Recht, J., Shales, M., Ding, H., Xu, H., Han, J., Ingvarsdottir, K., Cheng, B., Andrews, B., Boone, C., Berger, S. L., Hieter, P., Zhang, Z., Brown, G. W., Ingles, C. J., Emili, A., Allis, C. D., Toczyski, D. P., Weissman, J. S., Greenblatt, J. F., and Krogan, N. J. (2007) Functional dissection of protein complexes involved in yeast chromosome biology using a genetic interaction map. *Nature* **446**, 806–810
  39. Rhind, N., and Russell, P. (1998) Mitotic DNA damage and replication checkpoints in yeast. *Curr. Opin. Cell Biol.* **10**, 749–758
  40. Park, S., Isaacson, R., Kim, H. T., Silver, P. A., and Wagner, G. (2005) Ufd1 exhibits the AAA-ATPase fold with two distinct ubiquitin interaction sites. *Structure* **13**, 995–1005
  41. Wilcox, A. J., and Laney, J. D. (2009) A ubiquitin-selective AAA-ATPase mediates transcriptional switching by remodeling a repressor-promoter DNA complex. *Nat. Cell Biol.* **11**, 1481–1486
  42. Xie, Y., Rubenstein, E. M., Matt, T., and Hochstrasser, M. (2010) SUMO-independent *in vivo* activity of a SUMO-targeted ubiquitin ligase toward a short-lived transcription factor. *Genes Dev.* **24**, 893–903
  43. Pfander, B., Moldovan, G. L., Sacher, M., Hoege, C., and Jentsch, S. (2005) SUMO-modified PCNA recruits Srs2 to prevent recombination during S phase. *Nature* **436**, 428–433
  44. Moldovan, G. L., Dejsuphong, D., Petalcorin, M. I., Hofmann, K., Takeda, S., Boulton, S. J., and D'Andrea, A. D. (2012) Inhibition of homologous recombination by the PCNA-interacting protein PARI. *Mol. Cell* **45**, 75–86
  45. Armstrong, A. A., Mohideen, F., and Lima, C. D. (2012) Recognition of SUMO-modified PCNA requires tandem receptor motifs in Srs2. *Nature* **483**, 59–63
  46. Nakamura, T. M., Moser, B. A., Du, L. L., and Russell, P. (2005) Cooperative control of Crb2 by ATM family and Cdc2 kinases is essential for the DNA damage checkpoint in fission yeast. *Mol. Cell Biol.* **25**, 10721–10730
  47. Du, L. L., Nakamura, T. M., and Russell, P. (2006) Histone modification-dependent and -independent pathways for recruitment of checkpoint protein Crb2 to double-strand breaks. *Genes Dev.* **20**, 1583–1596
  48. Morris, J. R. (2010) SUMO in the mammalian response to DNA damage. *Biochem. Soc. Trans.* **38**, 92–97
  49. Morris, J. R., Boutell, C., Keppler, M., Densham, R., Weekes, D., Alamshah, A., Butler, L., Galanty, Y., Pangon, L., Kiuchi, T., Ng, T., and Solomon, E. (2009) The SUMO modification pathway is involved in the BRCA1 response to genotoxic stress. *Nature* **462**, 886–890
  50. Cremona, C. A., Sarangi, P., Yang, Y., Hang, L. E., Rahman, S., and Zhao, X. (2012) Extensive DNA damage-induced sumoylation contributes to replication and repair and acts in addition to the mec1 checkpoint. *Mol. Cell* **45**, 422–432